International Core Journal of Engineering Volume 11 Issue 6, 2025
ISSN: 2414-1895 DOI: 10.6919/ICJE.202506_11(6).0013

Design and Simulation of Tunable Vibrating Screen based on Eccentric Cam

Yifan Bai, Shengjie Zhao*, Xiongjie Liu, Huayu Huang, Xinyue Deng
School of Mechanical Engineering, Xi'an Shiyou University, Xi'an 710065, China
*13369348288@163.com

Abstract

As a commonly used screening equipment in industrial fields, vibrating screens are widely employed in petroleum, mining, pharmaceuticals, and other industries due to their high processing capacity, simple structure, and reliable operation. However, traditional vibrating screens face technical bottlenecks such as excessive vibrating mass, leading to increased demand for excitation force, higher motor energy consumption, and adverse effects on equipment lifespan. To address these issues, this paper proposes a novel vibrating screen driven by an eccentric cam mechanism, primarily composed of an eccentric cam, springs and their supports, screen mesh, and screen box. A three-dimensional model was established using Creo modeling software, and key parameters of the vibrating screen were determined. Dynamic equations for the eccentric cam were derived, and spring parameters were designed. Finite element simulation of the eccentric cam was conducted using ANSYS. Static analysis revealed a maximum stress of 34.917 MPa, significantly lower than the material's yield strength, and a maximum deformation of 0.0017 mm, confirming compliance with strength and stiffness requirements. Modal analysis indicated that the first six natural frequencies of the structure were well below the resonance frequency of the vibrating screen, ensuring resonance avoidance.

Keywords

Vibrating Screen; Eccentric Cam; Finite Element Simulation; Resonance.

1. Introduction

Vibrating screens, as critical equipment in manufacturing industries, play a vital role in screening operations across petroleum, mining, and food processing due to their simplicity, high efficiency, and stable operation. In the petroleum industry, vibrating screens serve as core equipment for drilling fluid treatment, enabling low-energy, high-throughput solid-liquid separation.

Research on screening machinery abroad dates back to the 16th century, with rapid advancements following the Industrial Revolution. For instance, high-frequency screening equipment developed overseas is widely used in coal slurry drying and grading processes. Countries such as Japan and the United States have achieved excellent results by applying dual eccentric axial excitation and synchronous belt transmission technologies in large circular vibrators. In recent years, wide-span triaxial vibrating screens showcased at international exhibitions demonstrate diversified development trends in screening machinery [1].

In China, the development of screening machinery has undergone three stages: import imitation, independent research, and technological enhancement. Due to historical limitations in industrial infrastructure and theoretical research, significant progress has only been made in the past five decades [2]. With industrial modernization, demands for screen variety and quality have increased, driving screening machinery toward standardization, serialization, and generalization [3]. To enhance screening efficiency, vibration intensity has been gradually increased while addressing environmental requirements (e.g., easy screen replacement and reduced dust leakage) and cost reduction through structural simplification [4].

Current challenges in vibrating screens include rapid screen mesh wear, severe noise pollution, and high motor failure rates. The root cause lies in the excessive vibrating mass induced by traditional drive systems, which escalates excitation force requirements, energy consumption, and structural fatigue. In view of the above problems, this paper proposes a design scheme for a vibrating screen driven by an eccentric cam mechanism. By separating the motor from the screen box, the mass involved in the vibration process is significantly reduced. Taking this new type of vibrating screen as the research object, the working principle analysis, feasibility argumentation, and structural parameter design are carried out.

2. Overall Design

2.1 Working Principle

A vibrating screen is a device that uses vibration force to achieve material screening. Its working principle is as follows: the motor excites the vibration of the screen body through a vibrator, causing the material to produce continuous jumping motion on the screen surface. The material is dynamically dispersed according to particle size, with larger particles remaining on the screen surface and smaller particles passing through the screen mesh into the silo [5]. The frequency and amplitude of the vibration force can be precisely controlled by adjusting the rotational speed and angle of the vibrator to adapt to the screening and classification needs of different materials. Additionally, the targeted design of screen mesh aperture size and shape further enhances the equipment's adaptability to diverse screening requirements. In practical applications, factors such as material physical properties, moisture content, and screen mesh wear affect screening efficiency. Therefore, equipment selection, screen mesh structure, and operating parameters need to be optimized according to specific working conditions, and fine maintenance should be implemented to ensure the equipment's efficient and stable operation.

2.2 Design Scheme

The proposed vibrating screen employs an eccentric cam mechanism (Figures 1 and 2). The screen box is mounted on a support base via springs, with eccentric cams embedded in grooves on both sides. The motor drives the camshaft to rotate, generating reciprocating linear motion of the cams, which in turn excites the screen box. Materials are classified through forced vibration, with oversize particles discharged via outlets. This design offers compactness, high efficiency, and broad applicability[6].

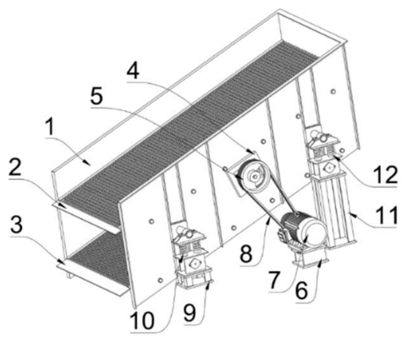

1-Screen Box; 2-First Screen Mesh; 3-Second Screen Mesh; 4-Cam Groove;

5-Second Pulley; 6-Motor Mount; 7-Motor; 8-Belt; 9-No.1 Spring Support;

10-First Spring; 11-No.2 Spring Support; 12-Second Spring

Figure 1. Schematic Diagram of the New-Type Vibrating Screen

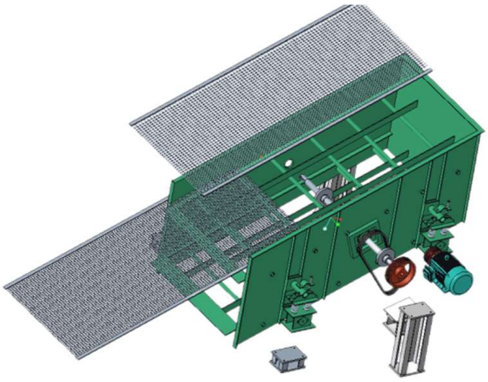

Figure 2. Assembly Model of the Vibrating Screen

Based on the contact form between the driving and driven members, eccentric cam mechanisms are divided into flat-top and sharp-top follower mechanisms. The contact point of the sharp-top follower mechanism is fixed, while that of the flat-top mechanism changes dynamically on the follower surface. Considering the working conditions of the vibrating screen, which require high load-bearing capacity, high-speed transmission, and good lubrication, a flat-top eccentric cam mechanism is selected. It offers higher durability, load capacity, and high-speed adaptability, effectively ensuring the working efficiency and operational stability of the vibrating screen.

The motor drives two eccentric camshafts to rotate at the same speed in the same direction, driving the cam grooves (screen frame) to perform reciprocating linear motion. The amplitude can be precisely controlled by adjusting the eccentricity of the eccentric cam. The screen mesh is fixed to the screen frame using an airbag support, and the screen frame is supported on the support seat by four sets of springs. The spring system has large elastic deformation and damping characteristics, which can effectively suppress the resonance phenomenon of the vibrating screen, reduce high-frequency vibration and noise, provide stable support during equipment startup and shutdown, and significantly reduce the resonance amplitude. The core advantage of this design is that the motor is fixed on the support seat and does not participate in vibration, fundamentally reducing the vibrating mass during operation. It features low power consumption, simple structure, stable operation, and low noise, showing good engineering application prospects.

2.3 Design Scheme

The design process of the vibrating screen includes key links such as setting design goals, determining basic parameters, optimizing dimensions, designing geometric parameters, and prototyping. The reasonable selection of basic parameters, including technical indicators such as screen surface inclination angle and screen hole size, is the core foundation of the design. After parameter determination, detailed design of components can be carried out.

Working parameters: The screen surface dimensions are length L=3.0 m; width B=1.5 m; number of screen layers is 2; screen body weight M_1=375 Kg; screen surface inclination angle $\boldsymbol{\alpha}$, defined as the angle$\boldsymbol{\alpha}$ between the horizontal plane and the screen surface. For vibrating screens used in screening, this angle ranges from 0°to 20°, with $\boldsymbol{\alpha}$=20°selected to balance screening efficiency and processing capacity. The vibration direction angleβcharacterizes the projection angle of materials on the screen surface, directly affecting material conveying speed and bounce height. Increasing this angle can improve screening efficiency but reduces throughput. A comprehensive consideration leads to selecting 45°to achieve an optimized balance between screening efficiency and production capacity.

The amplitude A refers to the maximum distance the screen surface deviates from the equilibrium position. Increasing the amplitude within a reasonable range can enhance material transport rate and promote particle ejection from the screen. A single amplitude of 7 mm is chosen to balance screening efficiency and equipment stability. The frequency ω is a critical working parameter of the vibrating

Volume 11 Issue 6, 2025
DOI: 10.6919/ICJE.202506_11(6).0013

screen. Appropriately increasing the frequency can reduce screen blinding and clogging, but excessively high frequency accelerates component wear and reduces screen life. With reference to the parameters of the ZD1530 vibrating screen, the vibration frequency n is determined to be 960 r/min.

Frequency:

$$\omega = \frac{2\pi n}{60} \tag{1}$$

Vibration intensity:

$$k = \frac{\omega^2 A}{g} \tag{2}$$

Throwing index D:

$$D = \frac{A\omega^2 \sin 45^{\circ}}{g \cos\alpha} \tag{3}$$

Participating mass:

$$\begin{aligned} M &= M_1 + M_2 \\ &= M_1 + K_m BL\gamma \sum H \end{aligned} \tag{4}$$

Excitation force:

$$F = MA\omega^2 \tag{5}$$

In the formula:

M_1 ---Vibrating screen quality,take 375kg; M_2 ---Material quality; K_m ---Material bonding coefficient,take 0.2; γ ---Bulk density,take $1500\,\mathrm{kg/m^3}$; $\sum H$---Total average thickness of material on each sieve surface,take 0.05 m.Substituting the data yields ω =100.48rad/s; k =7.21; D =5.43; M =442.5kg; F =31273.07N.

3. Eccentric Cam Design

In the design of the eccentric cam mechanism, a linear follower eccentric wheel mechanism is adopted to match the parabolic motion trajectory of the screen surface, as shown in Figure 3. This design can accurately adapt to the motion characteristics of the vibrating screen and effectively improve equipment performance [7].

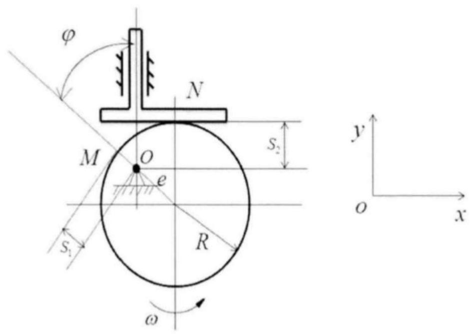

Figure 3 . Eccentric wheel geometric diagram

When the eccentric cam rotates from the initial position point M to point N, the geometric relationship yields:

$$S_1 = R - e \tag{6}$$

$$S_2 = R - e\cos\varphi \tag{7}$$

Follower push rod displacement:

$$S = S_1 - S_2 = e(1 - \cos\varphi) \tag{8}$$

Speed:

$$v = e\omega\varphi \tag{9}$$

Acceleration:

$$a = e\omega^2\cos\varphi \tag{10}$$

The deflection angle passes through 180°, the follower moves from the lowest point to the highest point, and the vibration undergoes 2 amplitudes, then S=2A=2e,so e=A=7 mm=0.007 m.

During the contact process between the eccentric cam and the cam groove, an external contact method is adopted [8]. Considering the operational requirements, this design selects 45 steel as the material for both the eccentric cam and the cam groove. The material properties are shown in Table 1.

Table 1. Material Parameters of 45 Steel

Parameter	**Density (kg/m³)**	**Modulus of Elasticity (GPa)**	**Yield Strength (MPa)**	**Poisson's Ratio**
45 Steel	7850	206	255	0.3

ISSN: 2414-1895 DOI: 10.6919/ICJE.202506_11(6).0013

For external contact, the contact stress is

$$\sigma_{\mathrm{H}}=\sqrt{\frac{\frac{\mathrm{F}}{\mathrm{B}}(\frac{1}{\rho_1}\pm\frac{1}{\rho_2})}{\pi(\frac{1-\mu_1^2}{\mathrm{E}_1}+\frac{1-\mu_1^2}{\mathrm{E}_2})}} \tag{11}$$

In the formula:

F---Total pressure acting on the contact surface,take 5565N;*B*---Initial contact line length,take 30mm;p_1---Eccentric cam material contact point curvature radius,take 60mm;p_2--The curvature radius at the cam groove material contact point,since the cam groove contact surface is flat,the curvature radius is infinite, take $1/\rho_2=0$;$\mu_1\mu$, $_2$---Eccentric cam and cam groove material's Poisson's ratio;E_1, E_2----Eccentric cam and elastic modulus of cam groove material.Substituting the data yields σ_H=416.4MPa.

Allowable safety factor S_n=1.3,Calculated as

$$\frac{[\sigma_{\mathrm{H}}]}{S_{\mathrm{n}}}=\frac{785}{1.3}=603.8\geq\sigma_{\mathrm{H}} \tag{12}$$

Meets the strength requirements [9].

Further analyzing the deflection of the eccentric shaft section, when only the excitation force is generated by the eccentric wheel vibration.

Deflection at the midpoint of the eccentric shaft segment:

$$w_1=\frac{5qB^4}{384\mathrm{EI}},q=\frac{F_1}{B} \tag{13}$$

Deflection at the midpoint under the action of eccentric blocks at both ends:

$$w_2=\frac{F_1BL_1{}^2}{8\mathrm{EI}} \tag{14}$$

Total mid-span deflection:

$$W=w_2-w_1=\frac{F_1BL_1{}^2}{8\mathrm{EI}}-\frac{5qB^4}{384\mathrm{EI}} \tag{15}$$

Set the midpoint deflection to 0:

$$L_1=\sqrt{\frac{5B^2}{48}}=9.68\mathrm{mm} \tag{16}$$

The vibration force and the spring support reaction force act on the screen body, causing it to undergo forced vibration. If the screen body moves synchronously and friction is negligible, the equation of motion is:

$$F = m\omega^2 e = \frac{\pi(2R)^2 B\rho}{4}(r-R)\omega^2 \tag{17}$$

Total kinetic energy:

$$E_K = \frac{1}{2}mv^2 + \frac{1}{2}J\omega^2 \tag{18}$$

Total potential energy:

$$E_P = \frac{1}{2}k{a_x}^2 + \frac{1}{2}k{a_y}^2 \tag{19}$$

Energy dissipation:

$$Q = \frac{1}{2}fa^2 + \frac{1}{2}f_0[(R-\cos\varphi)\times\omega]^2 \tag{20}$$

Total work done:

$$W = FA \tag{21}$$

Rotate the eccentric wheel to the equilibrium position, i.e., the deflection angle ω =90°,Follower acceleration a =0,speed v =0.703 m/s, f_0 =0.1,Then the total potential energy is zero.Then:

$$E_K + E_P + Q = W \tag{22}$$

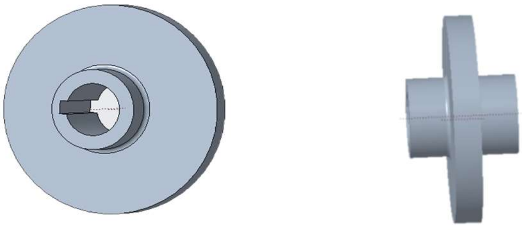

Figure 4. Eccentric cam model

Based on the above equations and substituting the data, the optimized structural parameters of the eccentric cam are as follows: radius R = 120 mm, thickness B = 30 mm, deflection radius r = 120 +

 Volume 11 Issue 6, 2025
DOI: 10.6919/ICJE.202506_11(6).0013

7 = 127 mm, connecting hole diameter with the drive shaft = 60 mm, length = 45 mm, wall thickness = 16 mm, eccentric cam mass m = 2.66 kg. The modeling is shown in Figure 4:

4. Spring Design

Among traditional support springs, cylindrical helical springs are selected as the support springs for the eccentric cam-driven vibrating screen for their economic practicality [8]. The working environment of the vibrating screen is complex, so silicon-manganese spring steel (60Si2Mn) Grade Ⅲ is chosen, which has excellent comprehensive properties. As the spring operates under ordinary load conditions, it is classified as Type Ⅲ. Referring to GB-T1239.6-1992, it can be obtained that the ultimate tensile strength of the material σ_b= 1570 MPa, yield strength σ_s= 600 MPa, elastic modulus E = 2.1×10^5 N/mm^2, shear modulus G = 7.8×10^4 N/mm^2. Since the number of load cycles exceeds 1×10^6, referring to the allowable shear stress for Class I loading, the allowable shear stress for 60Si2Mn material is: allowable shear stress [τ] = 628 MPa. F_{max} = 4451.2 N, F_{min} = 3367.07 N.

Calculate the wire diameter of the spring based on strength conditions. Currently, the spring index C=6 is selected.

Spring curvature coefficient:

$$K=\frac{4C-1}{4C-4}+\frac{0.615}{C}=1.25 \tag{23}$$

Correction value of spring wire diameter:

$$d\geq1.6\sqrt{\frac{F_{Max}KC}{[\tau]}} \tag{24}$$

Spring median diameter:

$$D=cd \tag{25}$$

Substituting the data yields K=1.25; d=12mm; D=72mm.

According to the national standard GBT1358-2009 for cylindrical helical spring size series, the first series is selected with d=12 mm, C=6, D=72 mm, K=1.25, meeting the requirement that C should be within the range of 4~8. Shear modulus G=8.2×10^4 N/mm^2

The compression method is used to determine the stiffness of the support spring, and the spring satisfies the following equation.

Stiffness:

$$K_z=\frac{F_{max}-F_{min}}{8} \tag{26}$$

Number of active coils in the spring:

$$n = \frac{Gd^4}{8D^3K_Z} \tag{27}$$

Actual axial stiffness:

$$K_1 = K\frac{n}{n_1} \tag{28}$$

Actual static deformation:

$$h = \frac{Mg}{4k'} = \frac{442.5 \times 9.8}{4 \times 116.55} \tag{29}$$

Substituting the data yields, K_Z =135.52N/mm; n =4.3t; ake n_1 =5;K_1 =116.55N/mm; h =9.30mm.

The modeling diagram of the designed support spring is shown in Figure 5, with its parameters meeting the dynamic characteristics requirements of the vibrating screen, providing crucial elastic support for stable equipment operation.

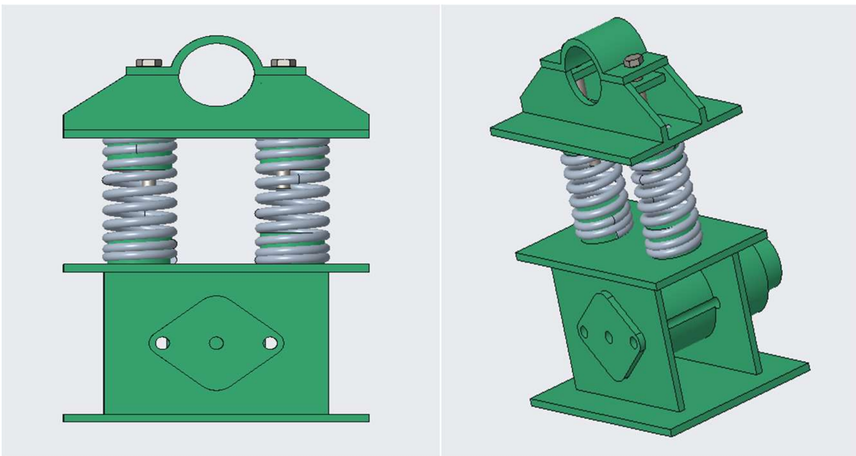

Figure 5. Support spring model

5. Static Analysis.

To verify the actual performance of the designed vibrating screen, it is necessary to conduct simulation analysis on its main mechanisms and observe whether the vibrating screen meets the requirements during actual operation [10]. The eccentric cam Creo model was imported into ANSYS Workbench for finite element simulation analysis.

5.1 Material Definition and Meshing

Considering the influence of excitation forces during the operation of the eccentric cam and comparing various material properties, the final material selection was 45 steel. The patch-adaptive method was employed to generate a tetrahedral mesh with an element size of 0.01 m, resulting in a total of 22,849 nodes and 14,469 elements. The mesh was inspected, and no negative volume elements [11] were found, with the mesh quality meeting simulation requirements.

ISSN: 2414-1895 DOI: 10.6919/ICJE.202506_11(6).0013

5.2 Static Analysis

During operation, if the eccentric cam undergoes significant deformation or fracture, it will severely impact the working efficiency and safety of the vibrating screen, necessitating static simulation analysis. The eccentric wheel must rotate around the shaft during operation, and remote displacement constraints are applied to restrict five degrees of freedom at the rotation center of the eccentric wheel, excluding rotation around the shaft. A vibration excitation force of 31,273.07 N is applied to the outer circumference of the eccentric wheel, resulting in the stress contour shown in Figure 6 and the deformation contour shown in Figure 7.

From Figure 6, it can be observed that the maximum stress occurs at the connection between the shaft and the eccentric wheel plane, with a peak stress of approximately 34.917 MPa, which is far below the material's yield strength, indicating no stress concentration. Figure 7 reveals that the maximum deformation occurs on the outer circumferential surface of the eccentric wheel, with a peak deformation of about 0.0017 mm. This minimal deformation will not affect the operation of the vibrating screen.

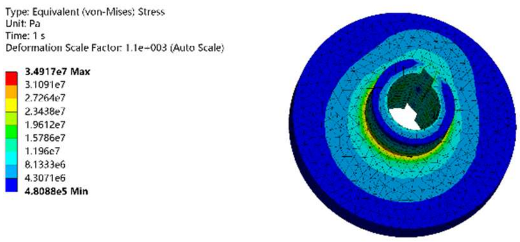

Figure 6. Stress contour map

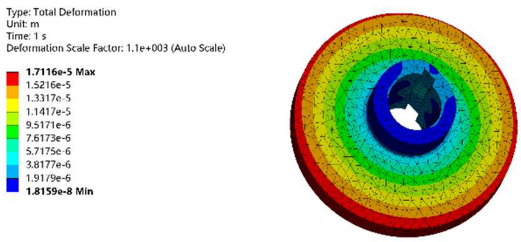

Figure 7. Deformation Cloud Diagram

5.3 Modal Analysis

Modal analysis is an analytical method based on structural dynamics, with the objective of obtaining modal parameters. By conducting modal analysis on a model, its inherent modes (frequencies, mode shapes) and corresponding modal parameters can be determined, thereby predicting frequency bands in which the system is susceptible to external vibration excitation. Resonance can be avoided by adjusting the system structure or other methods [12]. Performing modal analysis on the eccentric wheel allows observation of whether it resonates with the vibrating screen. The model is imported into the modal analysis, and the first six mode shapes are analyzed, yielding the first six modal analysis results as shown in Figure 8. The first six natural frequencies are 2375.4 Hz, 2523.9 Hz, 2783.1 Hz, 3029.3 Hz, 3190.7 Hz, and 3282.9 Hz, respectively. The resonance frequency of the vibrating screen generally ranges from 5 to 30 Hz. Since all first six natural frequencies are significantly higher than the vibrating screen's resonance frequency, resonance will not occur, meeting the design requirements.

ISSN: 2414-1895 DOI: 10.6919/ICJE.202506_11(6).0013

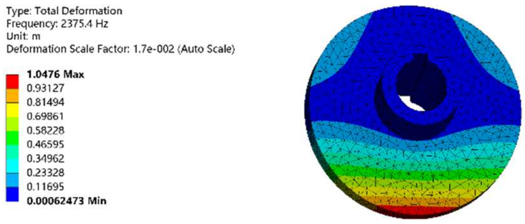

(a) First-order vibration mode

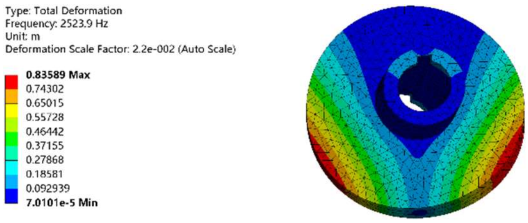

(b) Second-order mode shape

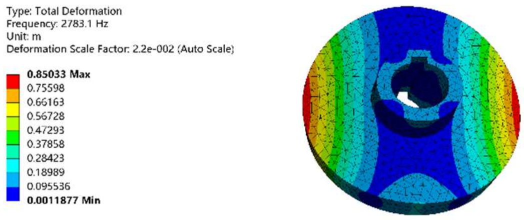

(c) Third-order vibration mode

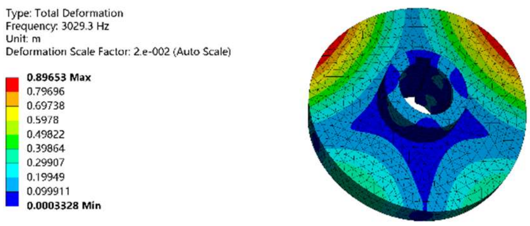

(d) Fourth-order vibration mode

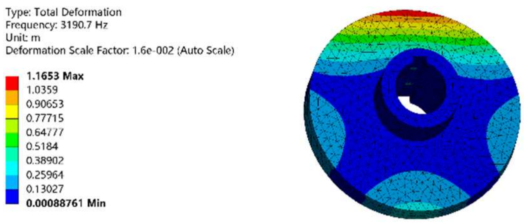

(e) Fifth-order vibration mode

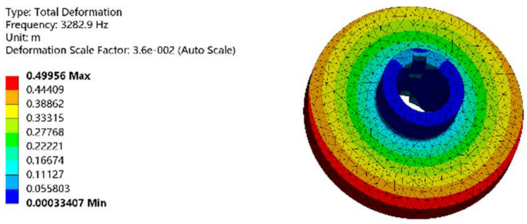

(f) Sixth-order mode shape

Figure 8. First six-order modal analysis results

6. Conclusion

This paper addresses the issue of excessive vibrating mass in traditional vibrating screens by proposing a novel design scheme driven by an eccentric cam mechanism. Through the separated arrangement of the motor and the screen box, the vibrating mass and energy consumption are effectively reduced. By analyzing the working principle and structural design, dynamic equations are established to clarify the motion laws, providing theoretical support for equipment optimization. Parameter calculations and component design verify the stability and efficiency of the proposed scheme. A 3D model is created using Creo, and finite element simulation analysis is conducted with ANSYS. The simulation results demonstrate that the eccentric cam meets the design requirements.

This study offers a new approach to the design of vibrating screens and provides theoretical foundations and data support. Future research could focus on optimizing the driving structure to overcome the limitations of linear vibration mode screens, exploring new mechanisms or vibration modes to enhance performance. Additionally, considering the interaction between materials and the screen mesh to refine the motion model could further improve screening accuracy and equipment reliability.

Acknowledgments

National College Students Innovation and Entrepreneurship Training Program 2023 (202310705009).

References

[1] Du X, Chen B. Development status and trends of vibrating screening machinery [J]. Science & Technology Information, 2010, (10): 109.

[2] Wang F. Development and prospects of screening machinery [J]. Mining Machinery, 2004, (01): 37–39.

[3] Duan Z, Guo B. Current status and development directions of vibrating screens in China [J]. Mining Machinery, 2009, 37(04): 1–5.

[4] Wen X, Akhter S, Afacan A, et al. CFD modeling of columns equipped with structured packings: I. Approach based on detailed packing geometry [J]. Asia-Pacific Journal of Chemical Engineering, 2007, 2(4): 336–344.

[5] Wu Z, Zhou C, Wu Y. Mechanism analysis of vibrating screens [J]. Sugarcane Industry, 1991, (05): 49–54.

[6] Deng M, Zhang G, Liang B, et al. Clay vibrating screen based on eccentric cam mechanism [J]. Journal of Mechanical Engineering, 2020, 15.

[7] Qu W, Tang H. Mechanical Vibration Handbook [M]. Beijing: Mechanical Industry Press, 1992.

[8] Guo N, Kuang Y. Research status and development of vibrating screens [J]. World Nonferrous Metals, 2009, (5): 2.

[9] Yang M. Dynamic model of high-speed cam mechanisms [J]. Machinery, 2007, 34(7): 4.

[10] Zhang S, Xu. Mechanical Components [M]. Beijing: Higher Education Press, 1981.

[11] Cheng Q, Xi W, Yan J, et al. Structural design and analysis of a dual-stroke wave energy converter [J]. Mechanical & Electrical Engineering Technology, 2025, 54(03): 52–57.

[12] Wei H. Dynamic response and noise analysis of electric angle grinders [D]. Suzhou University, 2014.